ISSN: 2690 - 0688

Research Article

Journal of Humanities & Social Sciences

A Robust Speech Features Extractor & Reconstructor For Artificial Intelligence Frontends

Ahmad Z. Hasanain[1*] , Judith B. Strother[2] , Marius C. Silaghi[2] , Veton Z. Këpuska[2] , Ivica N. Kostanic[2], Georgios C. Anagnostopoulos[2]

[1]College of Engineering at Al-Lith, Al-Lith, Kingdom of Saudi Arabia

[2]Florida Institute of Technology, Melbourne, United States of America

[*]Corresponding author

Ahmad Z Hasanain, Department of Electronics and Communication Engineering, College of Engineering at Al-Lith, Al-Lith, Saudi Arabia.

Submitted: 02 Aug 2022; **Accepted**: 11 Aug 2022: **Published**: 17 Aug 2022

Citation:Hasanain, A.Z., Strother, J.B., Silaghi, M.C., Kepuska, V.Z., Kostanic, I.N., Anagnostopoulos, G.C. (2022). A Robust Speech Features Extractor & Reconstructor For Artificial Intelligence Frontends. J Huma Soci Scie, 5(3), 230-245.*

Abstract

Human speech consists mainly of three components: a glottal signal, a vocal tract response, and a harmonic shift. The three respectively correlate with the intonation (pitch), the formants (timbre), and the speech resolution (depth). Adding the intonation of the Fundamental Frequency (FF) to Automatic Speech Recognition (ASR) systems is necessary. First, the intonation conveys a primitive paralanguage. Second, its speaker-tuning reduces background noises to clarify acoustic observations. Third, extracting the speech features is more efficient when they are computed together at the same time. This work introduces a frequency-modulation model, a novel quefrency-based speech feature extraction that is named Speech Quefrency Transform (SQT), and its proper quefrency scaling and transformation function. The cepstrums, which are spectrums of spectrums, are suggested in time unit accelerations, whereby the discrete variable, the quefrency, is measured in Hertz-per-microsecond. The extracted features are comparable to Mel-Frequency Cepstral Coefficients (MFCC) integrated within a quefrency-based pitch tracker. The SQT transform directly expands time samples of stationary signals (i.e., speech) to a higher dimensional space, which can help generative Artificial Neural Networks (ANNs) in unsupervised Machine Learning and Natural Language Processing (NLP) tasks. The proposed methodologies, which are a scalable solution that is compatible with dynamic and parallel programming for refined speech and cepstral analysis, can robustly estimate the features after applying a matrix multiplication in less than a hundred sub-bands, preserving precious computational resources.

Keywords: Pitch track; Pitch height; Normalized spectrograms; Language intelligence; Paralinguistics; Phonetics; Speech reconstructions

Introducton

At first glance at Figure 1, one can notice the parallel curves in the spectrogram of the human voice (Figure 1a) but not in the bird chirp (Figure 1b). The salient curly harmonics of the voice render a hidden state that appears contentious when connecting the dots. The speech spectrogram is a graph of the energy distribution along audio frequencies (i.e., the spectrum) versus time. The contrasts of the pictured graphs were adjusted per the CMYK printing norms; the higher the energies, the darker the pixels, but the color scheme can be reversed when printed on monitors. Human speech can be captured from the spectrogram using two features: the pitch and the harmonic intensities. In order to have artificial agents processing (or understanding) spoken languages naturally, it is crucial to realize a mathematical representation for speech that is attuned accordingly, especially because human intelligence and language are tangled up during development.

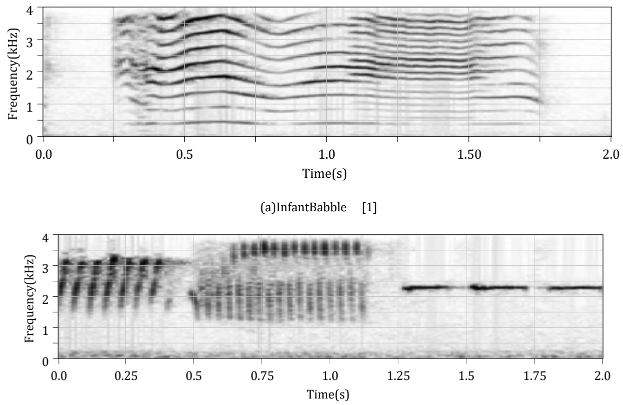

(a)InfantBabble [1]

(b) Canary Chirp

Figure 1: Spectrograms of Multi- and Mono-Resonance Communication Systems

The parallel curves that are shown in the spectrogram are generated by a locally-stationary signal. This means that the periodicity and the waveform shape fluctuate slowly, relative to the sampling rate. The local stationarity is proportional to the sharpness of the parallel curves. Speech producers flap in response to internal air pressure, air molecules are compressed and released periodically, and the pulse shape makes speech transmittable through air. The time distance between two adjacent compressions (bursts, pulses, or cycles) is the wave period (T_0), measured in seconds-per-cycle (1/Hertz). Equation 1 expresses the reciprocal relation between the wave-interval and the fundamental frequency, which is the frequency shift between two adjacent harmonic frequencies. This minimal shift is the speech fundamental frequency (FF or f_0). It is also called the frequency carrier and the pitch in some contexts. However, being in an air channel as its communication medium, the signal's actual periodicity is in meters per cycle. The λ_0 and υ in the equation are the corresponding wavelength and the speed of sound (in the medium). All variables are time variants. The υ is usually assumed to be constant although the temperature, humidity, and wind speed are not so along the air travel paths from the speech producer (vocal folds, cords, or glottis) to other human receivers.

$T_0 = \lambda_0/\upsilon = 1/f_0$ (second-per-cycle) (1)

In Figure 1b, the birdsong producer constrains its f_0 in a time-variant coordinate, which is then projected onto the two-dimensional spectrogram. The projection onto the periodicity space is non-linear since the f_0 teleports in the spectrogram as though two frequencies (e.g., 1 kHz and 4 kHz) are identical, because there are unaccounted independent axes. For example, the fundamental waveform of the canary bird is visually rotated around a variable axis parallel to the time axis, and its perimeter path renders a visual effect of cylinders in the figure. Assuming the bird's monotone was traveling with a constant angular velocity in a polar coordinate, the inferred radius of a pictured time-variant cylinder is about 1 kHz and centered at 2 kHz.

Similarly, the voice of the infancy in Figure 1a teleported back and forth between two speech depths during moments of emotional outbursts (e.g., between 1.25 and 1.5 seconds), which can be noticed in the audio playback. Per the juxtaposition of the two spectrograms, the human voice had a fundamental waveform, whose shape was transforming at a slow pace and had harmonic components, which rendered the parallel spectral curves. The tone-height-change phenomenon usually happens during puberty, and it doubles the fundamental interval, gears down the speech depth, and folds up the spectral code bandwidth. The speech resolutions happen accordingly. It is commonly known that deep human voices have been relatively overrepresented in the classic telephony bandwidth (4 kHz). It is also known that the spectral bandwidth scaling is an issue in Automatic Speech Recognition (ASR). In order to equalize the speech features extractions, more coordinates must be added.

The spectral energies of the harmonic components are the speech features. There are patterns that appear as if they were behind openings of window blinds. These patterns are called speech formants, and their mixtures make multitone phonemes. The harmonic components are also called timbre, overtones series, and cepstral coefficients. In this work, they are also the frequency envelope, the frequency-modulating signal, and the vocal tract response (H_m) for the purpose of mathematically modeling the speech signals and systems. Human speech consists of these components, which convey the hidden shape of the spatial cavities of the vocal tract (the nasal and oral cavities). The molecules' signals convolve with the vocal tract systems. The output of the modulating system is the speech signal, which, due to its local stationarity, consists of recognizable time units.

A 1989 study [2] suggested that human perception of speech relates to frequency demodulation. It also happens that two conventional approaches to pitch and speech feature extractions are modulation-based but applied to the frequency domain. Unfortunately, the classical frequency domain, albeit vital, made several speech modules hardly attainable. The speech modules that are needed are namely: pitch tracking and filtering, spectral depth normalization, and speech signal generation. Processing natural languages, for instance, the Generative Adversarial Networks (GANs), needs robust acoustic frontends that effortlessly unpack and compose speech utterances in a way that is similar to the natural extractors and producers.

A novel modulation-based approach is explained in this work for extracting the fundamental frequency and the harmonic energies, consisting of a speech model, a transform, and feature extraction methods. The approach is based on axiomatic assumptions: The voiced utterances are expressed in a variable speech resolution, and extracting the piloting f_0 makes the speech code instantly obtainable. Per the speech model, the human voice can consume less than 25.0 kilobits per second (kbps) of transmission bandwidth and is intelligibly recoverable when confined to less than a 4.1-kbps bandwidth. An overview, related work, and our contributions are in Section 2. Respectively, Sections 3, 4, and 5 outline the approach, the methodology, and the pitch-track-extraction results. The approach embraces two quefrency scales, a cepstral filter model, and cepstral processing measurements, and the quefrency transform and the speech feature extraction are described in the methodology section. Finally, the findings are discussed in Section 6, and a summary of the article and its implications are in the conclusion section (Section 7).

Review

The pitch extraction techniques are generally categorized into temporal, spectral, and cepstral approaches based on the processing domain: time, frequency, and quefrency. The quefrency is the frequency of frequencies and is the independent variable of the cepstrum, like the frequency is so of the spectrum. Even though several techniques had existed for pitch extraction [3], it still had drawbacks [4]. One of the time-domain methodologies is auto-correlation, which matches the speech signal with its lagged versions (as opposed to decomposing its independent frequency components). The frequency-domain is obtained in three operations: window slides, Fast Fourier Transform (FFT), and frequency banks. It is noteworthy that although the inverse Fast Fourier transform (iFFT) gives exact inversion theoretically, a Fourier transform defined over a finite interval is actually non-invertible, so its iFFT inverse is an estimation.

Like the frequency domain, the quefrency domain is a non-linear vector space, in which superposition does not hold. In the cepstrogram, the signals of the tract and the glottis become separable due to their characteristic differences. The cepstrogram is usually obtained from a high-resolution spectrogram along with two additional operations: logarithmic scaling (on both magnitude and frequency) and an iFFT. The iFFT is further approximated using the Discrete Cosine Transform (DCT) in the Mel-Frequency Cepstral Coefficients (MFCC) method. The cepstrum analysis [5] is defined as the power spectrum of the log magnitude of the power spectrum of the time samples [6]; i.e., Equation 2 or, equivalently, F^{-1}*log*|F{•}|, where F{•} denotes a forward Fourier transformation,√ *e−jθ = cos(θ) − j · sin(θ) [7, 8],* and set *j* = *pof* −1. In this work, the SQT domain emulates the set of the fundamental waveforms, which is a subset of periodic functions.
1 X2*cj*2π2*nmc* 1X2*cj*2π2*muc* 1

$$p[n] = \frac{1}{2c+1}\sum_{m=0}^{2c} e^{j2\pi\frac{nm}{2c+1}} log|\sum_{u=0}^{2c} e^{-j2\pi\frac{mu}{2c+1}} s[u]| \quad (2$$

For the pitch extraction, the Harmonic Product Spectrum is one of the most common methods, which De La Cuadra et al. [9] showed to be effective in adjusting acoustic instruments. Moreover, several methodologies in literature appeared promising, such as Pitch Contours (PC) [10], Amplitude Compression [11] (AC), and neighbor normalization [12]. However, David Talkin commented on the latter that its Normalized Cross-Correlation (NCC) amplified the ”peak at twice the correct period,” referring to what is called an ”A” tone. Figure 2a [12] shows three possible pitch tracks at 70 Hz, 140 Hz, or 210 Hz. According to the source, an NCC-based method was not instantaneously able to differentiate between the pitch and the two harmonically similar tones, which are apart at a one-unit-octave frequency. The ”almost perfect pitch tracker” of Ewender et al. [13] showed the challenge of the overtones still occurs in this century’s literature.

Another recent approach to speech features was the coherent modulation [14]; this method is known to be ”useful” when the modulating and modulated signals have commonalities. The coherent modulation was ”more effective than previously believed,” stated Clark and Atlas [15]. Particularly, Li and Atlas [16] outlined a detailed FFT-based procedure. Generally, the bulk of the algorithms in the literature perplex with the illusionary overtones because of the f_0 harmonic characteristic. Even human perception regards them as more similar than other tones, but human agents easily differentiate between each speech depth, implying that the ambiguity in f_0 should not exist in the acoustic frontend, rather at a deeper perceptual level. For instance, one could argue that harmonic illusion may have played a role in easing the language acquisition since it rolls the spectral code of the main speakers’ categories.

On the other hand, the frequency domain approaches are mediocre at limited computational power, and customizing.

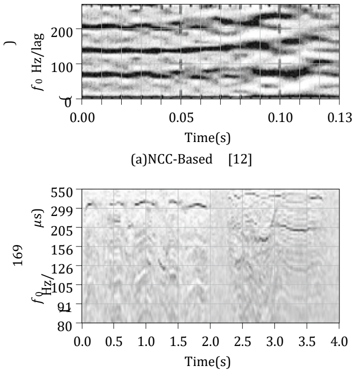

(a)NCC-Based [12]

(b) SQT-Based

Figure 2: Cepstrograms of Two Speech Feature Extractors

the conventional quefrency axis requires frequency banks. According to Moorer [17], the temporal and cepstral methods can complement one another as their features are approached differently. Unsurprisingly, the cutting-edge pitch trackers, such as Yet Another Algorithm for Pitch Tracking (YAAPT) [18], combine observation candidates from more than one pitch detection approach before smoothing the estimated pitch track. This combination comes with a computational cost, at which the sole cepstral approach is capable of producing fine pitch tracks.A possible workaround to this issue is to apply the process adaptively. Adaptive methodologies vary in the literature. For example, the overtone noise can be suppressed by a smoothing operator [19], which flattened the pitch track and, consequently, may have reduced the accuracy of the f_0 readings. The smoothing is an averaging operator that distorts acoustic information. It has to be replaced with non-linear filtering to preserve the original information recoverability. Several cutting-edge approaches have not been as robust as those for mammals, whose biological processors demodulate and compose speech signals effortlessly even though they operate at much slower processing speeds than today's machines.

SQT is novel and distinctive. Unlike the previous methodologies, not only does SQT extract recoverable harmonic spectra, but it also distinguishes the f_0 from its over- and undertones during the pitch extraction phase. Figure 2b depicts the cepstrogram of a multi-speaker channel. Before conducting the SQT-based extractions, male and female voices were added to an infancy voice background. The two persons had their f_0 in the quefrency ranges [80,155) Hz and [155,250) Hz, respectively, while the infant had its in the range [250,550] Hz. Theoretically, the addition of periodic signals is irreversible. However, each of the male and female utterances was still intelligible when "unmasked" or recovered from the other two voices in the background. This example illustrates the advantageous noise resilience of the proposed method. SQT has unique feature spaces, responsive normalizations, and quefrency scales. SQT extracts the speech features in practical means that can satisfy the required accuracy of any application. This is because applying Nyquist's theorem, which is usually applied on time axes, on the frequency axis suppresses the quefrency aliases. The outcome of this is analogous to the human ability to tune to one speaker and having the ambient noises blurred. In other words, SQT reduces the resolution of the background speeches. The other cepstral, spectral, and temporal approaches were either ineffective or computationally prohibitive when standing alone. They postpone complexities for later post-processing, since finding the speech model is not an easy task for unsupervised Machine Learning. In contrast, SQT facilitates relatively advanced capabilities for the artificial speech agents, such as simultaneously processing multiple and distant speeches.

Approach

Since the human acoustic sense is receptive to frequency-modulated tones, and because the vocal features are separable in the quefrency domain, it made sense to investigate the cepstral approach. Some may argue that not all human speech is periodical because there are phonemes that are unvoiced. However, the unvoiced phonemes still have a spectral presence and are partially detected by periodic filters. Additionally, the unvoiced phonemes are not entirely unvoiced. They are usually coupled by voiced segments to increase their air transmissivity. The unvoiced units are variations of noise, such as the violet noise, and can be modeled by smaller filters since they have smaller frequency resolution. Instead of adjusting two frame rates, another way to increase the unvoiced presence is to have the frame step no larger than 10 ms, or [0.010 · f_s] samples, where f_s is the sampling rate. The frame step is the time interval between similar points at two adjacent frames; it is also the complement of the frame overlapping. In other words, the sampled spectrograms can partially capture speech pulses and noises when the frame rate is increased due to its fast-paced transition. Note that, once the signal is in frames, the speech sequence is re-sampled from the sampling rate to the frame rate, f_r = 1/Frame Step or 100 fps (frames per second). The frequency domain is obtained from the quefrency selection on the SQT domain, which is obtained directly from the time frames.

This section presents logical intuitions and infers presumption axioms for the appropriate quefrency scale, the speech signal model, and the periodical cepstral measurement. The discussion also extends to the maximum window size.

Reciprocal Quefrency Scale

Cepstrum is a measurement of an acceleration rate, and its quefrency is equivalent to the change in frequency (Hz) per a time interval (μs). It may be misleading to count its unit in seconds although the unit can be expressed in samples ([20]). The proof that quefrency is the rate of change can be derived directly from intuitive definitions. Let the scalar quantities λ_0, *second*, and *second'* be sample measurements of the corresponding units cycle, s, and s', in some ϖ time unit. Since quefrency is the frequency of frequencies, but frequency is the rate of cycles per standardized second (hence, the rate of occurrence with respect to time), and since frequency also is, intuitively, the ratio of the standardized second to the comparable λ_0 interval (hence, $\frac{second\ \varpi}{\lambda_0\ \varpi}$in cycles/second or Hz unit), then similarly, quefrency is $\frac{second'\ \varpi}{second\ \varpi/\lambda_0}$ (in Hz-per-s' unit). That is, quefrency is the rate of (wave-period per the standardized second) per another constant second'; therefore, the unit of the quefrency is cycles per second squared if *second'* = *second.* In other words, although some equal quantities may be divided, their units are generally multiplied. For that reason, our reciprocal definition of the appropriate quefrency scale is
Equation 3, where f_{min} and f_{max} are the desired minimum and maximum quefrencies or f_0 boundaries, and $n \in \{0, 1, \cdots, N-1, N\}$.

$$R_{(n)} = R(n, f_{min}, f_{max}) = \frac{1}{\frac{1-n/N}{f_{min}} + \frac{n/N}{f_{max}}} \quad \text{(Hz/s')} \quad (3)$$

Consequently, the quefrency spacing is 1/Δq $\frac{f_{max}\cdot f_{min}\cdot N\times 10^{-6}}{(f_{max}-f_{min})}$ Hertz per microsecond (Hz/µs), and most importantly, since

$$\frac{1}{R_n}\text{(s'/Hz)} = \frac{1}{R_{n+1}}\text{(s'/Hz)} + \frac{1}{\Delta q}(\mu\text{s/Hz)}$$

then, the equivalent temporal unit is

$$\frac{(f_{max}-f_{min})\cdot 10^{6}}{f_{max}\cdot f_{min}\cdot N} \quad (\mu\text{s' =s)}$$

Notice the quefrency unit factor s' and the desired quefrency resolution *N* are inversely proportional.

Precisely, s' = $(f_{max} - f_{min}) \cdot 343 \times 10^2/(f_{max} - f_{min} \cdot N)$ centimeters when the speed of sound is 343 meters per second. The unit of the quefrency can be converted to samples given the sampling rate, as has been referred to. Notice that the Bark- and the Mel-scales, as well as the quefrency scale, exhibit logarithmic curves. One could hypothesize that the human reception of voice has a lower boundary (about 20 Hz/s') because of the reciprocal proportion, which spans quickly to infinity for the Direct Current measurement. Figure 3a shows the practical Reciprocal Scale (R-Scale), where the quefrency bins are spaced consistently such that Δq = Hz/36μs. On the other hand, Figure 3b shows the regular linear scale, where Δq varies from Hz/392μs to Hz/3μs. The two figures show cepstrograms of the same infant voices, whose pitches are in [190,480] Hz. The number of calculations was set constant to generate the two depictions, yet the linear scale is inefficient for several reasons. First, the frequencies around 100 Hz/s' of the regular cepstrum received exponentially low intensity, so they might underflow without a steep increase in computational resources. Second, the width of the pitch track and the energy distribution were not equal, and applying a post-processing process, such as frequency banks, on the already enlarged side of the scale, exacerbates the complexity. Third, normalizing the frequency scale after the fact adds uncontrollable noise to the pitch track because of the digitization happening at the intermediate phases. The common spectral approaches need more calculations to produce an imbalanced scale that requires the presence of another complexity that directly affects the readings' accuracy. On the other hand, placing the normalization up front equalizes the precision and boosts efficiency. See Figure 3a; the bandwidth (the line thickness) of the pitch track is consistent in the proposed R-Scale, and also obtaining the cepstral range from [150,500] Hz/s' consumed less than half the resources that would be necessary with the linear spacing. The quefrency ranges [110,220] Hz and [220,440] Hz get the same resolution when the two scales are weighted 70:30. The SQT scale is customizable per application.

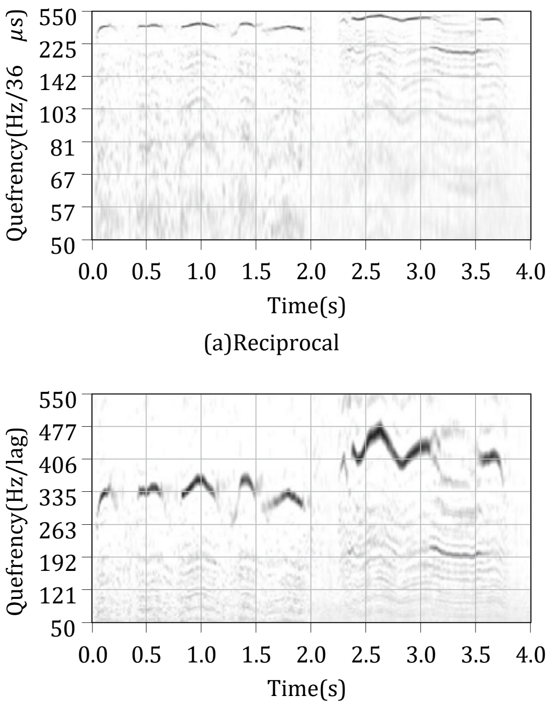

(a)Reciprocal

(b) Linear

Figure 3: Quefrency Scales

Window Size

Since the minimal pitch (f_{min}) is reciprocal to the maximal length of the wave-period, the f_{min} value is negatively proportional to the maximum window size, the frame interval of the sliding window. Note Equation 4 has m carrier signals (or frequency samples) that share the same phase and each is applied on a corresponding window $w_m[u]$ in the general case, taking the spectral leakage into consideration. When the quefrency scale is applied, $w_m[u] = w[u]$ for equal magnitude scaling; the harmonic components of an f_0 value must have the same window. Moreover, from the demodulation perspective, the quefrency sampling rate qs has to be at least double the frequency of the modulated signal. That is, based on the Nyquist theorem, at least two cycles must be measured for a reliable detection. The minimal sampling rate qs required to check if $cos(2\pi t \cdot f_0)$ exists without aliasing is $\frac{2}{f_0}$ Accordingly, the minimal length of the window is $(2c+1) = \frac{2}{f_{min}}$ seconds; equivalently, c ≥ $[f_s/f_{min} - 0.5]$ samples, where the [•] rounds up the • value to the nearest integer.

$$s[u] = \sum_m \underbrace{w_m[u,f_0] \cdot cos(2\pi \frac{u}{f_s} \cdot mf_0 - \varphi)}_{g[u]} * h[u,f_0] \quad (4)$$

There are three aspects to consider in determining the minimal quefrency. According to psychoacoustic experiments, human hearing may sense frequencies down to 20 Hz and does not discriminate between acoustic echos lagging less than 100 milliseconds [21]. Rarely does a speech signal have a frequency of less than 60 Hz, and these constraining values increase as one advances in age.

For most people, however, human perception is most responsive to the frequency band [1,5] kHz. Having said that, one should set the lowest measurable fundamental of the speech model to $f_{min} = 50$ Hz. This value sets the minimal frequency required to 25 Hz (this is approximately the lowest perceivable frequency to human beings) and the window length to 40.125 ms (less than the length of the ambiguity). Moreover, 50 Hz is the minimum frequency in most audio applications [22, p. 140]. The silence at 50 Hz corresponds to 40dB, at the lowest contour of loudness [23]. In summary, for an 8 kHz sampling rate, 321 subsequent samples are required in order to detect an event (e.g., impulse) that happens every 161 samples, and the shortest stationary unit of spoken languages takes more than 40 milliseconds.

Signal Model

Because speech is sampled, its harmonic sequence is bounded. The continuous speech signal is a random process whose random variables are the vocal tract and fold states. The two have physical limits safeguarding their characteristics from abrupt changes. This makes speech presentable in frames. Let each time frame have ($2c$ + 1) subsequent samples such that the discrete time axis is $u \in \{0,1,\cdots,2c\} = Z[0,_{2c}]$. Let a harmonic number (also called order, rank, or term) be $m \in \{1,2,\cdots,M\}$, where M is the highest desired harmonic order. In addition, let a set of fundamental frequencies have indices $n \in \{0,1,\cdots,N\}$. The variable lengths N, M, and c are non-negative integers (Z+) and are utilized in Section 4.2. To obtain the signal model, it is of interest to formulate a quefrency transform $T : \mathbb{R}^{(2c+1)}_{[-1,+1]} \longrightarrow (\mathbb{R}^{(N+1)}_{[f_{min},f_{max}]}, \mathbb{R}^{M}_{+})$

that maps the ($2c$ + 1)-sample vector to an (N + 1)-quefrency × M-harmonic matrix.

Without loss of generality, consider the situation where only one glottal signal and one vocal tract system generate the time frame. The speech is a time variant whose waveform can be modeled with wavelets. Needless to say, the harmonic multiplicities are embedded within the f_0 waveform, which is a variable function. However, in the ideal case, the glottal signal is a unit impulse train, whose Fourier transform is a train of impulses, re-scaled to $2\pi f_0$ magnitude (noted later in Equation 8). The idealization of the basic waveform g[u] spreads its f_0 into harmonics with equal magnitudes. Now, placing four formants on that harmonic medium can be obtained when the impulse train passes through a multi-bandpass filter, whose impulse response function h is actually the shape of the waveform. The convolution happens as the filtering tract system responds with a time sequence at every stimulus it receives. Moreover, due to the speech depth phenomenon, the filtering system (h) is a nonlinear function of f_0. In general, a speech time frame is modeled as Equation 4, where the summation is over the harmonics, the convolution (*) is the filter operator, and the φ is the instantaneous phase, usually in the range [0,2π] radians. However, since the phase is considered only for synchronization (minimizing the angular difference between the signal transmission and the filter reception), and because the output of interest is the absolute magnitude, its effective range becomes $[0,\frac{\pi}{2}]$ radians, and an absolute value operator is added for the other half. The function $\varphi[\omega]$ for the d-index phase $\omega = \{0,1,\cdots,d-1\}$ is defined in Equation 5 for completion.

$$\varphi[\omega] = \frac{\pi\omega}{2(d-1)} \quad (5)$$

A practical enhancement to reduce the spectral leakage is to define the time-frame windowing $w[u,f_0]$, controlling the widths of the harmonic banks because the default window is square if the shape is not defined. The frequency response of the window substitutes each sinusoid filter with a continuous range of sinusoids, resulting in a relatively wider band at mf_0. The windowing also attenuates the energy magnitudes exponentially. The Dolph-Chebyshev function is one of the unique windows because it has an almost flat spectral attenuation. In other words, the additive distortion of the Chebyshev window is roughly distributed uniformly, enhancing the performance of a subsequent maxima detection. Framewise, the windowing operator is linear and reversible as long as its entries are positives. The Chebyshev window is achieved per the desired width of the main lobe and an iFFT application. Applying the Stone-Weierstrass theorem, the windowing generates polynomial functions that realize approximated cosine functions on the bounded bandwidth. Keep in mind that the equality of Parseval's theorem is defined on rectangular windows.

Given the equation of the main-lobe width defined by Smith [24], one may obtain Equation 6, which calculates the level of attenuation (A) in decibels (dB), having a frame length ($2c$ + 2) and a main-lobe side width w_b. From the cepstral perspective, the spectrum of $h[u,f_0]$

($H_m[f,f_s]$) $q_s = \frac{1}{f_0} \le \frac{1}{f_{max}}$ is sampled at (in harmonics per Hz). Crystallizing the definition of the quefrency unit of the previous section, the application of Nyquist's theorem on the quefrency domain makes the spectral width less than or equal to $2f_0$; i.e., $2w_b \le 2/q_s$. The desired width is $w_b = f_0/|2\kappa - \sigma|$, where $\sigma \in [0.5,1.5]$. When $\sigma = 0.5$, the model is resilient to noise, and when $\sigma = 1.5$, the model is enhanced in noise-free environments. Since most Chebyshev implementations require the attenuation, the included equation is handy. The default value of σ is 1.0. Equation 7 defines a Gaussian-based alternative window. Most importantly, estimating the energy after the transform is possible only when the samples of the window sum to one. Finally, an obvious best practice is to have the windowing operation applied once to the SQT matrix rather than to every input frame.

$$x_0 = 1/cos\Big(\frac{\pi}{f_s} \cdot \frac{f_0/2}{|2\kappa - \sigma|}\Big)$$
$$A = 20 \cdot log_{10} cosh\big(2c \cdot cosh^{-1}(x_0)\big) \quad (6)$$

$$W_g[u] = exp\Big(-\frac{(u-c)^2}{cf_s/f_0}\Big) \quad (7)$$

Cepstral Measurement

To derive the harmonic sampling, first apply the Fourier transform to Equation 4 to obtain Equation 8, where $W_m[f,f_0]$ is the window's frequency response. (Let $W_m[f,f_0] = Wm[f]$ and $Hf,f_0 = H[f]$ since the non-linearity of H is discussed later in Section 6). After rearranging the terms, the glottal frequency response is Equation 9.

$$S[f]=2\pi f W_m[f,f_0] * \underbrace{\sum_{m\in Z} \delta(f-mf_0)\,e^{j\varphi}}_{G[f]} H[f,f_0] \qquad (8)$$

$$G[f]=\sum_{m\in Z} W_m[f-mf_0]=\frac{S[f]\cdot e^{-j\varphi}}{2\pi f\cdot H[f]} \qquad (9)$$

The formants are much wider than the harmonic samples in G, so the energy of H is approximately non-varying within ± $\frac{f_0}{2}$. Therefore, $H[mf_0] \approx H[mf_0 \pm \frac{f_0}{2}$], and at $f = mf_0$ ± , $\frac{f_0}{2}$ the $S[f]$ becomes the tract signal $H[f]$ plus some noise. The additive noise is sizable in the signal-to-noise (SNR) ratio because the impulse response is attenuated in that region. That is $H[mf_0 \pm \frac{f_0}{2}] = S[mf_0 \pm \frac{f_0}{2}] \pm \epsilon$, and the spectral energy at mf_0 is

$$\begin{aligned} G[mf_0] &= \max_{\varphi} \frac{S[mf_0]\cdot e^{-j\varphi}}{2\pi f_0 \cdot H[mf_0]} \\ &\approx \max_{\varphi} \frac{S[mf_0]\cdot e^{-j\varphi}/2\pi f_0}{S[f_0(m-\frac{1}{2})]\cdot e^{-j\varphi}+\epsilon} \end{aligned}$$

Since the detection of f_0 depends on the M harmonic observations, the detection probability $Pr[f_0]$ is equivalent to $Q_m\ Pr[mf_0]$. Likewise, the cepstral similarly, $P[f_0]$, is equivalent to $Q_m\ P[mf_0]$. The calculation is usually preferred in decibels for several reasons. Also the adjacent harmonics should be multiplied to filter out the undertones. The addition operation is computationally safer than multiplication, and underflowing can be avoided with a stabilizing $\epsilon = 0.001$. The logarithmic option is also more time efficient than the multiplication when the log conversion of the matrix entries is applied in parallel. However, the log operation can be substituted by a fractional exponent. One of the possible cepstral measures $P[f_0]$ is therefore defined in Equation 10. Overall, the intensity of the quefrency correlates positively with $^{Q}{}_{m}$ $|S[mf_0]|$ and negatively with $Q_m\ |S[(m^{-0.5})f_0]|$. The relation between them can be either a signal-minus-noise value or a Signal-to-Noise Ratio (SNR), and the subsequent detection can be done with either maxima or minima. This section covered the basic mathematical intuitions, and the next section uses the inferences.

$$\begin{aligned} P[f_0] &= \prod_{m} |G[mf_0]| \equiv \sum_{m} \pm\max_{\varphi}\{\, 20log_{10}|\epsilon + S[mf_0]e^{-j\varphi}| \\ &\mp 20log_{10}|\epsilon + S[f_0(m-0.5)]e^{-j\varphi}| \\ &\mp 20log_{10}(2\pi f_0)\,\}\ \text{(dB)} \end{aligned} \qquad (10)$$

Methodology

Having had the signal model of Equation 4, the quefrency measure in Equation 10, and the context of the previous section, this section applies the SQT matrix T, which is applicable on the frames $s[u]$, to obtain the desired speech features $S[f]$.

Notation

Let $(N + 1)$, M, and $(2c + 1)$ be the numbers of quefrencies, harmonics, and time samples respectively. The variables N, M, and c are user-defined integers larger than one. Also f_{min} and f_{max} are variable f_0 boundaries, where $f_{min} < f_{max}$. Additionally, let $d \in \{1,2,4\}$ be a selectable phase synchrony mode, where the complexity levels 1, 2, and 4 correspond to real, complex, and sliding-phase types of detection. In terms of notation, let $s(t,u)$ be the uth time sample in the t^{th} frame of N frames, and so s is an $(N + 1) \times (2c + 1)$ matrix. In Equation 10, label the first cepstral signal S (of the modeled numerator) with $\kappa = 0$ and the second S (of the noise) $\kappa = 1$. Then, the first and second $S[f]e^{-j\varphi}$ of the equation can be expressed in a 5-d matrix, Equation 11. Now, an entry of S is equivalent to a vector product between a time frame and a slice of the transform. That is the matrix multiplication $S = s{\cdot}T$. The next section describes how to build and use a transform such as the one in Figure 4.

$$|S(t,n,m,\omega,\kappa)| = |s(t,\forall u) \times T(\forall u,n,m,\omega,\kappa)| \qquad (11)$$

Transformation

We define the T of SQT and its instantaneous frequency $f(n,m,\kappa)$ as follows:

$$T_{(u,n,m,\omega,\kappa)} = \frac{W_{(u)}\cdot cos\left(2\pi\frac{(u-c)}{f_s}f_{(n,m,\kappa)} + \varphi_{(\omega+d)}\right)}{\sum_u |W_{(u)}|} \qquad (12)$$

$$f_{(n,m,\kappa)} = R_{(n)}\cdot(1+m+\psi(R_{(n)})-\kappa/2) \qquad (13)$$

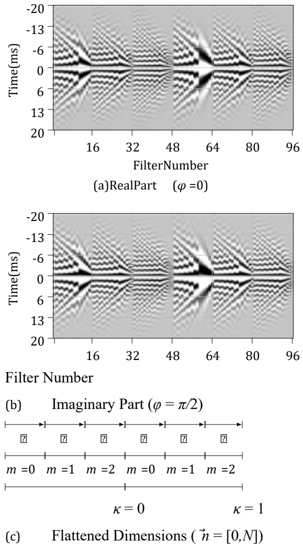

(a)RealPart (φ =0)

(b) Imaginary Part (φ = π/2)

(c) Flattened Dimensions ($\vec{n} = [0,N]$)

Figure 4: SQT Matrix

The R and φ are N-lengthed and d-lengthed vectors, obtained from the scale definition in Equation 3 and the instantaneous phase definition in Equation 5. W is a $(2c + 1)$-lengthed vector of a Chebyshev window with an attenuation of Equation 6. The frequency-shift function ψ is defined in Equation 19. The time index u was shifted by c and the phase index was shifted by d for filter centering. Table 1 completes the definition of the transform. In practice, the transform is constructed using matrix manipulations on Mesh Grid coordinates. It may also be necessary to flatten (or vectorize) the dimensions 2-5 in low-level programming language.

For the general description of the transform, Figure 4 depicts the real part and imaginary parts of a flattened matrix example, $T_{(u,\cdots,\kappa)}$. The depiction visualizes a stack of scallops rather than cochleas. The real part is even with respect to time, while the imaginary part is odd, so it is symmetric about the time origin. The vertical axis is the frame's interval in seconds. The first set of 48 filters along the horizontal axis corresponds to $\kappa = 0$ (the numerator S), and the remaining set of 48 filters corresponds to $\kappa = 1$ (the denominator). The difference between the two sets of 23: **end procedure** 24: functions is the scale with respect to time. In the two sets, the first 16 filters are of $m = 1$ (the first harmonic, the f_0), the next 16 filters are of $m = 2$ (the second harmonic), and the last 16 filters are of $m = 3$. The 16 filters in each are $n \in \{0,\cdots,15\}$. In the general case, the first axis corresponds to the time samples of windowed sinusoids. The second dimension varies the sinusoids' frequencies according to the quefrencies, and the third varies per the harmonic overtones. The last two dimensions are for detection enhancement via phase synchronization and alias cancellation. The transform is applied on stationary frames. The output of the transform is a stochastic process that conveys three random variables: the periodicity, the envelope, and the noise. They are necessary to detect the quefrency f_0, which shifts the modulating signal H_m.

Table 1: SQT Generation

```
INPUT: $f_s = 8000, f_{min} = 100, f_{max} = 300, N = 15, M = 3, c = 160, d = 2, \sigma = 1.0$ - parameters
OUTPUT: $T, R$ - quefrency transform and scale
procedure SQT($a,b$) ▷ generates the transform if it is not in memory.
$T \leftarrow$ zeros( $(2c+1)\times(N+1)\times M\times d\times 2$ ) ▷ initializes the transform matrix with zero values
$R \leftarrow$ zeros( $N+1$ ) ▷ initializes the quefrency scale of the transform
$f \leftarrow zeros((N+1)\times M\times 2)$ ▷ allocates temporary matrix space
$W \leftarrow$ zeros( $N+1$ ) ▷ allocates temporary vector space
    for $n \in [0,N]$ do
        find $R_{(n)}$                                        ▷ using Equation 3
        for $m \in [0,M-1]$ do
            for $\kappa \in \{0,1\}$ do
                Calculate $f_{(n,m,\kappa)}$                  ▷ using Equation 13
                if $f_{(n,m,\kappa)} \le f_s/2$ then
                    Calculate $W_{(n)}$    ▷ given the main-lobe width of $0.5R_{(n)}/|2\kappa-\sigma|$
                end if
                for $u \in [0,2c]$ do
                    for $\omega \in [0,d-1]$ do
                        Calculate $T(u,n,m,\omega,\kappa)$    ▷ using Equations 12 and 19
                    end for
                end for
            end for
        end for
    end for
    return $T,R$          ▷ used together: $T$ extracts the spectral values at $R$
```

Speech Feature Extraction

The sampled time frames are projected onto a three-dimensional feature space during the transformation. (See Equation 11). We theoretically demonstrated that including two extra axes (i.e., ω & κ) was a necessity for reliable quefrency readings. To obtain the visioned 3-D speech space, apply absolute magnitude, synchronize by either a max operation or a summation along the ω axis, as in Equation 14, and extract the $\kappa = 0$ matrix slice. The $S(\bullet_{,n,m,\kappa=0})$ resembles a monochromatic 2-D time-frame, where the n and m are the indices for the quefrency rate track $f_0(t)$ and the normalized spectrograms $H_m(t)$.

$$S(t,n,m,\kappa) = \max|S(t,n,m,\forall\omega,\kappa)| \qquad (14)\ \omega$$

To calculate the cepstrogram measurements of Equation 10, apply a log or fractional exponent operator, flip the sign where $\kappa = 1$, and aggregate the κ and m terms. The log operator of the noise-canceling stage is not required, but pre-processing it with a 4-adjacency filter can bridge the transitioning between the connected pixels instead of significantly distorting the extracted information with the smoothing operator at the end.

$$P(t,n) = X\ (-1)\kappa \cdot 20log10S(t,n,\forall m,\forall\kappa)\ (dB)(15)\ m,\kappa$$

The f_0-levels (or indices) with the highest score estimate along the n-axis are extracted with the arguments of the maxima (*arg max*), as in Equation 16a. Given the f_0 track, the vocal tract responses (H_m) are extracted by applying the indices to Equation 16b. The f_0-levels at t/f_rs are then converted to the Hertz unit by the R-Scale of Equation 16c, since the f_0 axis is quantized earlier per the reciprocal frequency scale R (of Equation 3). Finally, Table 2: Validation Results of Preliminary Data the f_0 and Hm are the extracted speech features.

$$r[t] = argmax[P_{(t,\forall n)}] \qquad (16a)$$

$$Hm[t] = S(t,n=r[t],m,\kappa=0) \qquad (16b)$$

$$f0[t] = R(n=r[t]) \qquad (16c)$$

Results

A preliminary comparison between three pitch extraction implementations is in Table 2. The Quefrency Transform Twelve (QT12) is one of our Matlab implementations based on the SQT method (defined in Table 1). The other two pitch extractors are formal Matlab implementations based on the Pitch Contours (PC) and the Amplitude Compression (AC), which are briefed in Section 2. According to Matlab, the two implementations are not entirely based on the proposals "A Pitch Estimation Filter

Robust to High Levels of Noise (PEFAC)" and "Automatic Speaker Recognition Based on Pitch Contours" by Gonzalez et. al. and Atal respectively. GPE (Gross Pitch Error) is a common speech metric of pitch performance. A smaller GPE value correlates with better methods. It is the probability the error threshold is exceeded. GPE-20 is the probability of obtaining an absolute-value error over the threshold of 0.20 or 20% of the target label. The statistical significance validation was applied to the Matlab reference audio file ”Counting-16-44p1-mono-15secs” with 0dB additive noise of ”Turbine-16-44p1-mono-22secs.” The SQT matrix had 12 harmonic components, hence, QT12. Its complexity was adjusted so that it equals the sum of the complexities of the MFCC’s and PC’s implementations, since the SQT features are comparable to the features of both MFCC and PC. The table shows that the time complexity of the QT12 was lower than the AC’s complexity and higher than the PC’s. Also, the GPE of QT12 was lower than the PC’s error and slightly higher than the AC’s. Generally, the FFT spectrogram had the lowest computational complexity. Note that the features of FFT and the QT12 are recoverable. That is, the SQT technology can be utilized for AI speech composition and speech synthesis. However, the features of MFCC and FFT do not produce pitch tracks. This section continues with a detailed pitch tract evaluation of the three Matlab functions.

Pitch Extraction Evaluation

Table 3 prints out performance metrics of three methods under several noise conditions, totaling 28 tests. QT mostly had the lowest probability of Type-1 error when the significance thresholds were set to 20% and 10%. QT and PC were neck and neck when the threshold was set to 5%. The proposal evidently outperformed the other two methods in all of the additive noise conditions that were tested: noise-free, white-noise, and turbine-noise. AC generally performed well when the turbine-noise level was high, and PC generally did so when the white-noise level was low. The evaluation shows that the pitch detection performance of the proposed method performed excellently. Another indication for the pitch accuracy is the speech quality of the reconstruction. It may be safe to assume that QT is relatively robust in high noise conditions.

Table 2: Validation Results of Preliminary Data

Features	Recoverability	Time	GPE-20
PC	N/A	0.046	6.589
AC	N/A	0.127	5.448
QT12	Yes	0.058	5.740
MFCC	No	0.012	N/A
FFT	Yes	0.007	N/A

Test Samples

Figure 5a demonstrates the SQT approach in practice, whereby higher frequencies were assigned fewer quantization levels. Figure 5b plots the samples of two waveform signals: the original and its twelve-tone reconstruction. The composition is no small feat, and its Root Mean Square (RMS) envelope is fair. The speaker traits, like accent, however, were less present, and that was expected since only a dozen components were extracted for this set of tests.

Experimental Settings

The selected evaluation dataset was called Frequency Determination Algorithm (FDA) Evaluation Database [25]. The fundamental frequencies of the FDA data are labeled at a 20 kHz sampling rate of a 5.53-minute audio of male and female speakers. To increase the difficulty of the pitch extraction, the sampling rate of the data was decreased to 8 kHz. The results were recorded at the minimal lag per method to decrease the implementation delay differences. A median filter whose size is three was appended the f0 extraction processes, which were conducted online in the Matlab platform (2019b) [26]. The average feature-extraction times for the SQT (this article), AC [11], and PC [10] methods were 1.34, 3.24, and 1.16 seconds, respectively. The QT was constructed with Gaussian windows and $M = 12$, the first five of which were used for the pitch detection.

Table 3: Test Results of the FDA Data

Settings		methods	Error Metrics				
			Lag	GPE-20	GPE-10	GPE-05	RMSE
No Noise		QT	0.00	2.18	5.84	14.34	25.44
		AC	0.00	4.34	8.03	18.28	45.84
		DC	0.00	3.65	7.88	15.77	34.73
White-Noise	dB20	QT	4.97	2.24	6.30	14.82	27.26
		AC	11.00	4.40	8.92	19.08	48.88
		DC	0.50	3.66	8.28	16.38	34.42
	dB10	QT	0.97	2.66	10.32	18.81	38.68
		AC	37.65	5.13	15.63	26.30	74.95
		DC	29.87	3.91	13.67	23.25	44.97
	dB0	QT	3.00	6.74	6.13	14.61	25.42
		AC	56.40	11.89	8.39	18.51	45.77
		DC	66.30	9.15	8.09	16.00	34.22
Turbine-Noise	dB20	QT	4.39	2.46	6.13	14.61	25.42
		AC	12.50	4.66	8.39	18.51	45.77
		DC	16.10	3.80	8.09	16.00	34.22
	dB10	QT	11.74	5.70	9.3213	17.532	32.11
		AC	33.71	8.45	12.36	22.46	51.24
		DC	59.71	7.55	11.89	20.23	41.14
	dB0	QT	27.81	30.23	34.23	41.08	61.51
		AC	35.30	30.34	34.99	45.68	77.97
		DC	45.10	37.33	41.86	48.83	80.32

The metrics are variant significance testing cases and a squared loss case; the gross pitch error (GPE), its lag, its significance (GPE-Threshold), and the Root Mean Square Error (MSE) are defined in Equation 17. Two types of noise signals, white noise and turbine noise, were added in three SNR cases: low (20dB), medium (10dB), and high (0dB) noise conditions. The metrics of the tests involving randomness are represented by the average of 30 repetitions; each was determined at the most suitable GPE lags.

$$\text{GPE} = \frac{1}{T}\sum_{t=1}^{T} |\hat{f}_0[t] - f_0[t]|$$

$$\text{Lag} = \frac{1}{F_s}\underset{\Delta t}{argmin}\sum_{t} |\hat{f}_0[t-\Delta t] - f_0[t]|$$

(17)

$$\text{GPE-}\xi = P(\ |\hat{f}_0 - f_0| > f_0 \cdot \xi/100\ )$$

$$\text{RMSE} = \sqrt{\frac{1}{T}\sum_{t=1}^{T} |\hat{f}_0[t] - f_0[t]|^2}$$

Discussion

This section discusses the limitations and analyzes the implications of the results. The results show that the speech intonation is indeed an essential feature. The pitch patterns are essential for emotion expression and recognition. However, they has been absent from the state-of-the-art speech synthesizers. For example, the voices in the OpenAI project hardly express any emotions. Furthermore, since the pitch unit is expressible in Hertz-per-microsecond, our cycle acceleration perspective is not only valid intrinsically but also mathematically. Additionally, the results show that the SQT pitch tracks are objectively superior to the recent alternatives in the Matlab toolbox. Also the SQT feature engineering is clearly robust in its feature reconstructions. Finally, the limitation of the study is that it included just two pitch track extractions, two quefrency scales, and two datasets. First, the two pitch track extractions were apparently better than several other pitch extractions under preliminary test conditions, so the two were most likely representative of the methods in the literature but not necessarily so. Second, there might be scales other than the linear and the reciprocal spaces. For example, a trade-off between the two scales might be better than the reciprocal scale. Third, the harmonic shift may have been caused by the equipment, so it may not be from the source of the voice. Therefore, future work can include recordings of multiple microphones. Other recommendations for follow-up research include machine learning, multi- and distant speech recognition, and some of the communication parts were briefly mentioned in this article, which has supplementary audio files [27]. For example, the MFCC and the SQT hyperspace can be compared in the speech emotion classification. Another example is that the deep learner may auto-encode speech signals using the reconstruction speech formula. The remainder of this section provides technical elaborations in retrospect to the previous sections. A case study highlights the findings, the end product, and the significance of the fundamental frequency for speech signal processing.

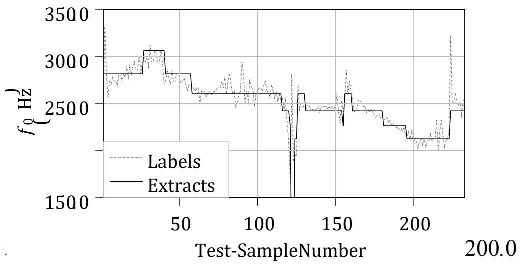

reciprocal spaces. For example, a

(a) Pitch Track

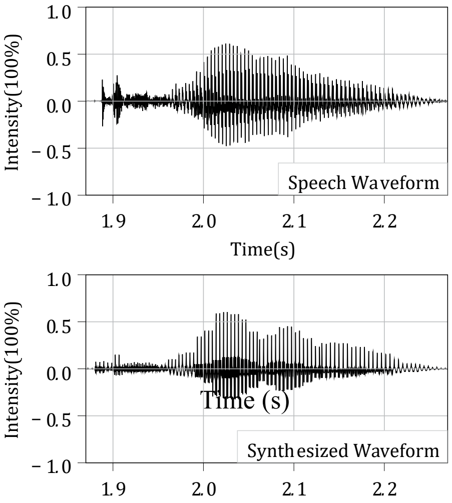

(b) Speech Reconstruciton of a ”Car” Utterance

Figure 5: Illustrative Example from the FDA Data

Speech Depths

The medium of the air particles is equivalent to a low-pass channel; it attenuates the high frequencies of the utterances. Speech audio is also anti-aliased (or low-pass filtered) while it is acquired and stored. Because higher FFs spread the cepstral code to higher frequencies, each speech depth naturally has a speech resolution, not to be confused with the frequency resolution. The depth must be one of the f_0 coordinates. The speech features correspond to the average of the repeated shape in the periodic series. It can be modeled as $h(t,f_0)$ on the time domain, in which it exhibits a variation of a sine cardinal function, i.e., sinc, or modeled as $H(f,f_0)$ on the frequency domain, in which it can be approximated by Gaussian Mixture Models. The variability of the speech depth may have fostered communications within household members and facilitated language learning along one of the speech dimensions, since each speech depth happened to have a speech resolution and a cepstral band, and since a simple projection can align the speech features of different speakers' characteristics. The speech depths are commonly associated with masculinity, femininity, and infancy. However, the overall majority of human beings naturally produce the resolution that is also a common characteristic of the youth voice.

Newborns first encounter blurred speech, and the low resolution perhaps helps humans acquire and model languages in a gradual general-to-specific heuristic search, guiding the internal neural systems. Generally, increasing f_0 prioritizes the voice over the voices with lesser ones; this is ascribable to the voice masking phenomena, which is caused by the fact that two time periods of a high f_0 resemble a time period of a low f_0, but not vice versa. (The utterances consist of pulse wavelets rather than sinusoids). For example, requiring more signal processing filters and listening to a conversation whose background is voices of unsatisfied dependents require extra mental work to filter out high f_0 interference. The unpleasant noise may further the survival of the species, preventing child neglect. On the other hand, lowering the f_0 expands its voice coverage since signals traveling on lower frequencies optimize their energy for long distance communications (like in open fields). Although the gender may have a degree of correlation because of the vocal folds' lengths [28],

The association does not hold because of the existence of sizable minorities, which makes the majority of human voices have high pitch. Moreover, the voice generator can transit between the speech resolutions regardless of sex and age. For instance, parents tend to use infant-directed speech to promote communication and learning. The findings of [29] showed showed that infants who babble at an early age receive contingent feedback from social interactions that foster language learning. Likewise, infants can produce adolescent-directed speech. The illustration of Figure 1 about the phenomena affirms previous speculations in the literature. For example, [30] and [31] mentioned that consensus of the two-dimension view of f_0 was motivated by auditory expertise.

One may speculate about the underlying physical constraints that prompt the λ_0 doubling; however, the teleport path, which is shown in Figure 3, indicates that the f_0 has an additional dimension. A rotation around the second axis is called the height of the pitch and is believed to be 110 Hz, although this number is not exactly the same for every human being, especially with the environmental influence. A 2017 survey by Bernhardsson [32] in Github showed that the arithmetic population mean of f_0 varies per language. Moreover, similar to speech production, human perception of speech does not considerably discriminate between the intonations that are one octave apart. The term pitch implies the angular position, while the f_0 refers to the measurement reading. The relation between the two terms is expressed mathematically in Equation 18: the f_0 is congruent to the pitch modulo height. $f_0 \equiv \text{pitch} \pmod{\text{height}}$

$= \text{pitch} + \text{height} \cdot \text{depth}$

$$\text{height} \approx 110 \quad \text{depth} \in \{0.5, 1, 2, 4, 8\} \qquad (18)$$

Case Study

Figure 7 prints the spectrogram of four Wake-Up-Word (WUW) utterances from the WUWII Corpus [33]. The utterances are, from left to right, a female voice of ”Voyager,” a male voice of ”Voyager,” another male voice of ”Operator,” and another female voice of ”Operator.” The last utterance ends with a noticeable tone. Each waveform of the four was normalized by its extrema before they were concatenated. Comparing the H_m (i.e., timbres) of the four utterances, one may notice a shift in the intensities of the overtones. Based on the shift within the Mel-scale, a harmonic shift ψ can be approximated as in Equation 19. Figure 6 shows a partition of the frame data.

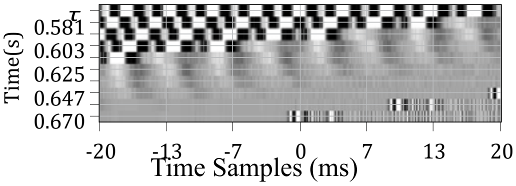

Figure 6: Speech State Transition From a Phoneme at frame τ To a Pulse at 0.670 (s)

Applying the transform (T) on the frames s (as in Equation 15) gives the normalizing sampled spectrogram S and the cepstrogram P. Applying Equations 16a and 16c on the cepstral similarity extracts the f_0 path.

$$\psi(f_0) = max\left\{0, \left\lfloor \frac{700}{f_0} - \pi \right\rfloor \right\}, \quad (f_{c}\text{Hz/s'}) \qquad (19)$$

Figure 8 renders two cepstrograms of two configurations: fast (Figure 8a) and boosted or refined (Figure 8b). The common paramters of the two cases are f_{min}:100, f_{max}:300, c:160, d:2. The first option is economical in terms of its resource consumption (and faster than the latter). The configuration parameters of the first are N:7, M:3, Shift:0, σ:1.5. Observing three overtones (M = 3) turned out to be adequate for the pitch estimations (in a low-noise setting). The size of its matrix transform is 321 × 96. On the other hand, the parameters of the boosted configuration, whose transform size is 321 × 320, are N:15, M:5, Shift:ψ, σ:1.0. Considering more harmonic observations (M = 5), the second generates f_0 readings that are sharper than the readings of the fast configuration.

The detection of the pitch track in Figure 8a has larger variances than the pitch track in Figure 8b. The large variances are due to the reduced quefrency resolution. Reducing the number of bins (N + 1) reduces the time complexity. Meanwhile, the refined results in the boosted case have a relatively large number of quantization levels, increasing the precision of the readings. It is worth noting that the refined cepstrgoram can be composed of two smaller ones; hence, the output quality can scale up with dynamic programming or boosting techniques.

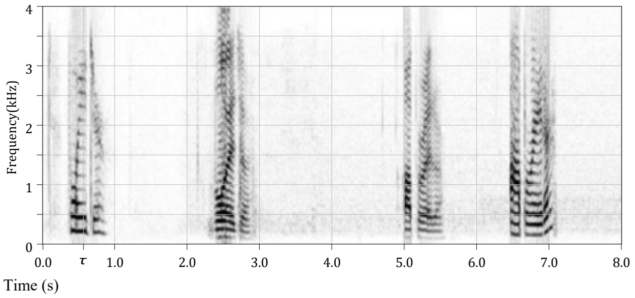

Figure 7: Spectrogram of Two ”Voyager” and Two ”Operator” Utterances [33]

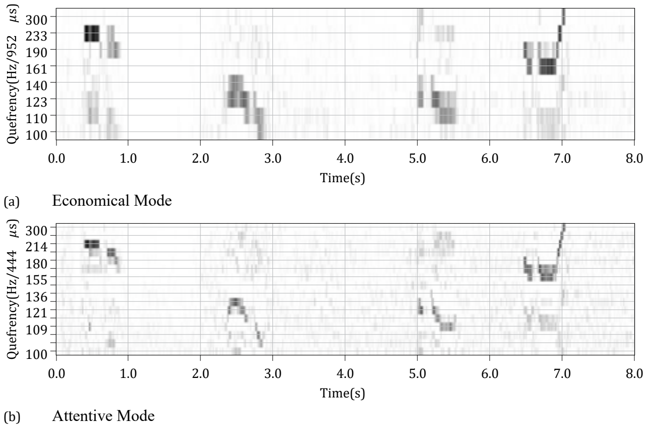

(a) Economical Mode

(b) Attentive Mode

Figure 8: Cepstrograms’ Complexities

Additionally, one may notice that speech closure pulses can be located from the sharp pitch patterns, and so averaging (smoothing) the pitch track was avoided so as not to distort the speech signals. Moreover, the path can be rendered discontinuous in the unvoiced intervals by applying a voice activity detection that utilizes the extracted pitch energies along the most vivid track. The extracted cepstrgorams illustrate that the voiced samples of different depths are linearly separable in the quefrency domain. Two speakers utilized the quefrency channel between 155 and 300 Hz/s’, and two other speakers utilized the channel between 100 and 155 Hz/s’.

In another similar example, the first and last two seconds of the case study (Figure 7) were added to the babbling (Figure 1a), and a high definition quefrency transform (sized 321 × 4096 with N:63, M:16, and σ:0.5) filtered the utterances from the congested audio signal that has three voices at a time. The cepstrgram of that example is demonstrated in Figure 2b. The intelligibility of the recovered speech correlated with the f_0 as was expected. Nevertheless, based on Parseval’s theorem, the total energy in the time domain is comparable with the aggregated spectral energy, as in Equation 20. The Root Mean Square (RMS), preferred for describing the audio time-frames, is the square root of energy. The theorem holds true only when the applied windows are rectangular, so the proximity in the equation occurs when the frames and the transform are windowed. Also, the right hand side is the L^2-norm of H_m since the denominator is already considered in the windowed transform (Equation 12). Figure 9 plots the two sides of the proximity to illustrate the energies of the extracted pitch tracks. It shows that the increased number of harmonics along with the harmonic shift ψ increased the extracted pitch RMS and energies. The voice activity can be detected from the boosted case (Figure 9b) better than from the swift extraction (Figure 9a).

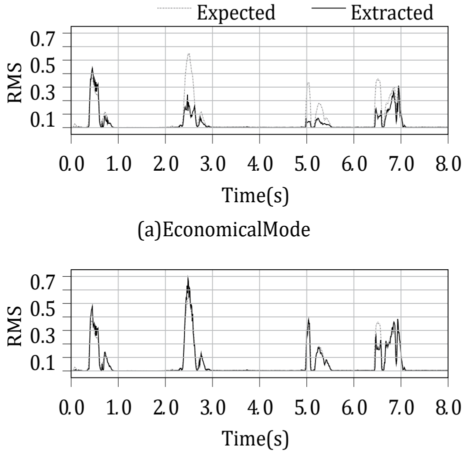

(a)EconomicalMode

(b) Attentive Mode

Figure 9: Energies of Total and Pitch Extractions
[!p]

The extracted samples, which compose a harmonically normalized spectrogram Hm, are depicted in Figure 10 for each of the two cases. Given the signal model (of Equation 4), $f_0[t]$, and the two $H_m[t]$, speech signals were reconstructed, and their regular spectrgorams are depicted in Figures 11. The depictions show that the extracted harmonic elements were placed back to their spectral locations. One can see that the discrete shift skips a few harmonic elements in the second and third voices to normalize the frequency scaling of the vocal tract. It is worth noting that the correlation between the f_0 and the tract is a correlation between two glottal characteristics.

$$RMS_{(t)} = \left|\sum_u \underline{s}^2_{(t,\forall u)}/(2c+1)\right|^{\frac{1}{2}} \approx \left|\sum_m H^2_{(t,\forall m)}\right|^{\frac{1}{2}} \quad (20)$$

The more harmonic overtones, the higher the speech quality. If the minimal quefrency of the speech model is

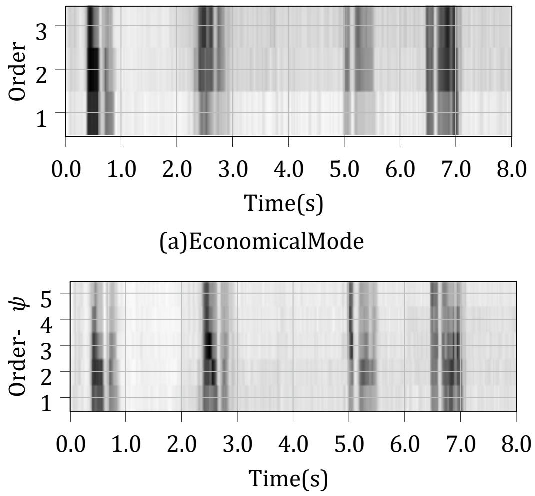

(a)EconomicalMode

(b) Boosted Mode

Figure 10: Spectra Features (*H_m*)

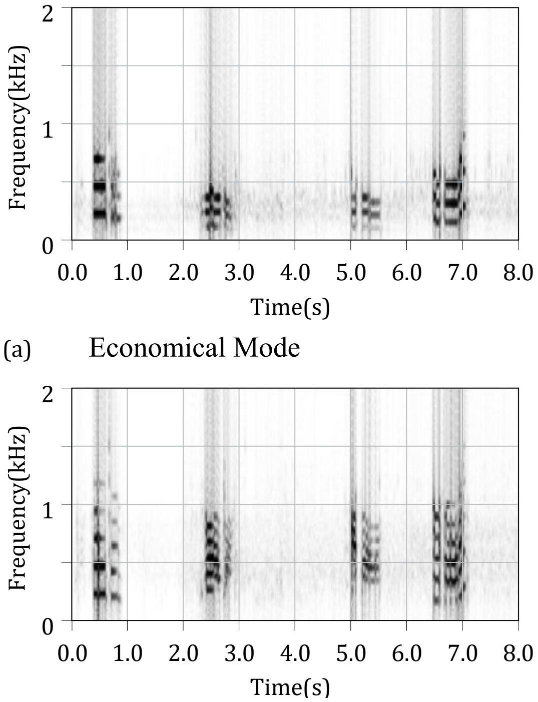

(a) Economical Mode

(b) Boosted Mode

Figure 11: Spectrograms of Reconstructed Speech Signals f_{min} = 50 Hz, the maximal number of overtones within the bandwidth $\frac{f_s}{2}$ = 4 kHz is $\lfloor \frac{f_s/2}{50} \rfloor$ = 80. Figure 12a depicts all H_m components in 4 kHz, and its corresponding spectrogram reconstruction is in Figure 13a. It recovers a spectorgram approximation of the original input signal (Figure 7). Another configuration is to subsample the speech spectral code to$\lfloor \frac{f_s/2}{330} \rfloor$=12 features as in Figure 12b. This reconstruction can be intelligible with a large number of bins.

The first two speech formants are within the first 16 overtones, as shown in Figure 13a. Needless to say, the significance of the harmonic digit decreases as the harmonic rank increases. Also, the f_0 is included in the figure as the smallest tone. Since the first two utterances correspond to the wake-up-word ”Voyager,” while the last two do so to ”Operator,” one can conclude that the high depth adds extra speech details that may not be essential in differentiating between the two speech utterances. Consequently, only the first speech features are usually considered. For example, the MFCC method includes the first 13 cepstral coefficients. However, in the standard MFCC procedure, the overtones with high ranks are averaged or interfered with. This is because its Mel-Scale is applied to the downsampled spectrograms, shown in Figure 13b. For that reason, the MFCC does not align the harmonic ranks. In the figure, the eight harmonics of the first utterance are mapped to the fifteenth harmonics of the second utterance. One possible normalization is depicted in Figures 12c and 13c. The normalization aligns the similar features of the similar utterances by considering an equal number of harmonics. Additionally, the ψ function increased the normalization even more, and it became more resilient to the quantization error than the subsampling of Figures 12b and 13b. Finally, digitized 8-level H_m and 32-level f_0 may be sufficient for machine learning. If the number of harmonics (*M*) is 12 and the frame rate is f_r = 100fps, the two levels aggregate to *(M · log2(8) + log2(32))* · f_r = 4.1kbps (kilobit-per-second), which is a reduced transmission bandwidth.

Spans of Language and Intelligence

The generation and recognition of spoken languages are sophisticated processes. Since the intelligence of a species can function as a means of its survival, the two processes can be genetically optimized during a lengthy selective reproduction phase, as languages interconnect with and boost intelligence. For example, having been bestowed control over their own breaths, species like dolphins, elephants, and birds have been able to extend their senses beyond their lines of sight and share alerts and information within the kind. For instance, whales communicate at long distances and navigate their surroundings, transmitting sound units and receiving sonar echos. The utilization of the spoken units is a founding module for intelligence just as the human utilization of written alphabetic and numerical symbols is a basis for written knowledge, commerce, and civilization. Human languages come in several forms, and each has a countable number of units (or letters). In the spoken one, the phoneme is the unit of speech.

The ability to understand logic and the ability to comprehend a sequential series of events must have been, to a certain degree, built upon the primal ability of recognizing sensory data, such as speech processing. The former ability is equivalent to the latter ability when the domain of the speech spans multiple days as opposed to minutes. Some may argue that some individuals learn to walk first while some talk first. Even so, human language acquisition begins much earlier with quasi-resonant vocalizations, according to Psychologist Rachel [34]. Moreover, according to Linguist Noam [35], there exists an innate Language Acquisition Device (LAD) in the human brain that pre-positions the ability to acquire linguistic concepts, such as nouns and verbs. It is true that the tuneful pattern is not exclusive to humans; however, the speech ability has been vital to humankind [36]. Our hypothetical reasoning is that graceful recognition of temporal sequences also enabled the comprehension of the more-complex sequences that have many events. When these were optimized (in succeeding iterative genetic mutations), intellect possibly emerged naturally in the species. Constituting a self-aware agent, hierarchical spans of language are levels for intelligence. Increasing the contrast of visualization can extend the attention spans hindered due to developmental disorders [37]. Additionally, magnetic resonance imaging (MRI) has revealed that both the processing of language and the ability of using tools stimulate similar neural areas [38]. Undoubtedly, speech signal processing is part of decision-making processes.

Having been blessed with automation, human populations flourished. For instance, individuals merited more labor rights when steam engines were employed in the agriculture industry, but the recent technological leaps may require safe domestic machines that add the human component to the autonomous world. Since the acoustic agents (or companions) are expected to comprehend meanings and interact not only intellectually but also to form bonds with human agents, the artificial agent would first have to receive and generate a voice in a similar manner to humankind, although not necessarily by biological means. A human-like learning phase may occur in digital systems with a specific signal acquisition formula.

Paralinguistic Intonation

To obtain natural speech utterances, the harmonic features have to be combined with natural f_0 patterns, which can be regarded either a discontinuous or a continuous discrete function $f_0[t]$, as in Figure 14. The fundamental frequency (f_0) is the main speech feature, vital in natural language processing, especially in languages where speech stresses play a major role in defining the speech parts and grammar. Additionally, modeling English grammar would lean on the $f_0[t]$ patterns.

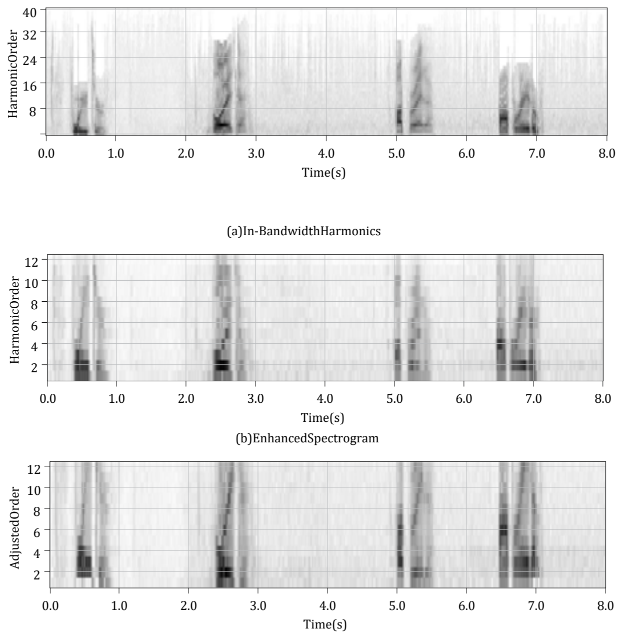

(a)In-BandwidthHarmonics

(b)EnhancedSpectrogram

(c) Normalized Spectrogram (H_m)

Figure 12: Comparison Between Frequency Sampling Configurations

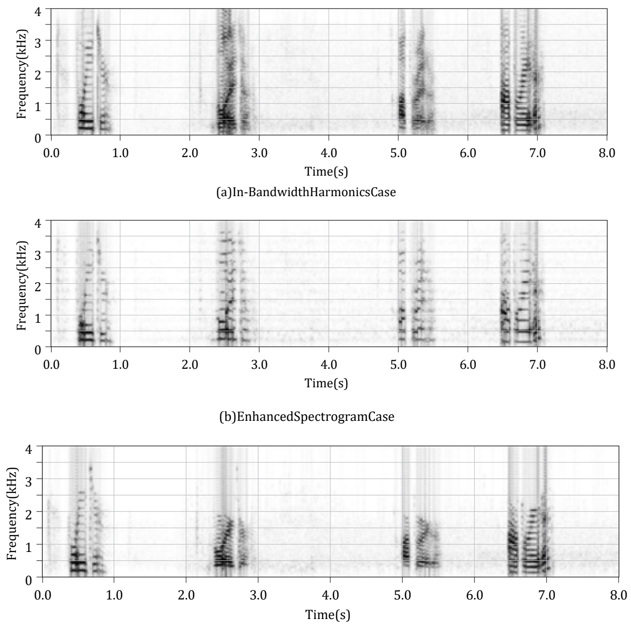

(a)In-BandwidthHarmonicsCase

(b)EnhancedSpectrogramCase

(c) Normalized Spectrogram Case

Figure 13: Spectrograms of Reconstructed Speech Corresponding Respectively to the Cases in Figure 12

Intonation patterns, sometimes marked with diacritics, are essential in word recognition and are common in Eastern languages. According to Albert [39], the vocal communications may convey four times more information than the verbal communications. For instance, the double consonants in the Korean language such as: ga, ka, and gaa, are written differently because they represent different vocal track states. However, because of the frequency modulation, gaa naturally has higher voice components than ka and ga have according to Sun [40]. In other words, the cepstral domain is more expressive than the spectral domain. Other examples are the tashd¯ıd emphasis in Arabic, the acute accentuation in Greek, and the compound words in English. For instance, the stressed syllable in ”thermometer” is just as important as its phoneme sequence. Moreover, the regular pattern of the f_0 is a reduction since it correlates with the breathing pattern. For instance, adults breath slower and so naturally do their glottises move more slowly. The general pattern was shown in previous publications, according to which also the emotions, such as happiness and sadness, correlate with the pitch pattern [41]. Utterances normally de-accelerate toward local minima. In contrast, f_0 increments appear while appending upcoming expressions. The f_0 function holds clues for several grammar components: punctuation periods, clauses, and stresses. A persistent upward trend may imply a preparation; the accelerating is salient in the regularly de-accelerating pattern. Exclamation points and question marks are slightly similar; the former is a (linear) trend across the utterance, while the latter is an f_0 suffix (usually an exponential one). Additionally, the speech emphasis is a short up-down bounce, which is the most frequent pattern. A varying f_0 can possibly grasp attention as the auditory focuses of the listeners are more likely to intersect with the speaker's tone. Such an intersection maximizes the reception of the speech. That is, words uttered with bouncing tones do sound emphasized as they widen in the quefrency domain. Ample pitch patterns would have to be analyzed for conclusions.

The verbs and the nouns have different syllable stresses although they may have similar phoneme sequences. The utterances of neutral statements and wake-up-word requests diverge naturally in the f_0 pattern. The f_0 highlights some parts of speech, and this is crucial for machine learning and language understanding. This is because the f_0 is a primary component in natural languages.

Conclusion

This work refines the quefrency definition as a unit of acceleration, measured in Hz/μs, and the f_0 is a primary speech feature, not separable from the spectral energies. While the commonplace frequency banking does not make the MFCC features reconstructable, the proposed method adjusts the frequency banking implicitly in the frequency responses of the windows to make the features reconstructable. The cepstral domain is adequate when it is configured as in the proposed approach since the windowing operator convolves with the frequency domain and attenuates its magnitudes exponentially. Furthermore, the proposed method calculates the pitch and its spectrum at the same time; it is more efficient than an equivalent combination of other state-of-the-art methods.

The findings confirm experts' speculations, such that the f_0 has two dimensions: depth height and intonation class. The two dimensions are considerable because speakers sometimes gear between the depths almost instantly. While the depth determines the speech resolution, the intonation is crucial for Natural Language Processing (NLP) and Wake-Up-Word (WUW) systems since it communicates urgency and breath patterns. The speech resolutions are the result of the stationarity, the speech depths, and band-limited speech channels, limiting the number of the speech components.

The f_0 intonation clues primitive language. It may be evident that the language expressed in the intonation precedes the shaping capability of the vocal tract. Like facial expressions, the pitch patterns could be prehistoric and universal. The proposed approach addresses several challenges in order to elevate speech processing to the comprehending level. It is crucial that ASR systems effortlessly detect and compose speech in resolutions that conserve energy, optimize the features' SNR, and preserve the speech components during extraction.

The proposed Speech Quefrency Transform (SQT) is suitable for artificial intelligence processing. The proposed method achieved a relatively very low Mean Square Error (MSE) via the frequency demodulation assumption. The transform expands the speech samples into a hyperspace whose axes correspond to pitch, harmonic spectra, and frequency-based anti-aliasing. The intent of the dimension expansion is to increase the data separability for the speech cluster analysis. Whenever the ASR is attuned to an f_0 carrier, the quality of the extract is high since the background noise is attenuated. Distant- and multi-speech detection and extraction are expected to be more feasible with the provided method. For example, a heuristic acoustic model may cache recent utterances to gradually increase observations as language and contextual models require for an observation instance. For fast processors, the first five harmonica, in which the first formant usually resides, are sufficient. For speech normalization, the first twelve harmonica, conveying the first two speech formants, are so. The method is compatible with high performance computing since it consists of matrix operations. The SQT method attenuates the background noise, and its input can be reconstructed.

Statements and Declarations

We have no conflicts of interest to disclose. The datasets that support the findings of this research are available from Dr Paul Bagshaw and Minnesota Department of Health (MDH). However, the data is available from the corresponding author upon reasonable requests and permissions from the cited authors.

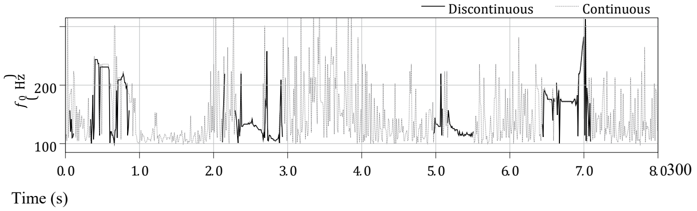

Figure 14: The Pitch Track of the example in Figures 12a (Discontinuous) and 12c (Continuous)

References

1. Minnesota Department of Health. DataSample 4: Baby Behavior. Youtube. a 2020;https://youtu.be/EYe0ee2-uS4.
2. Stefanatos, G. A., Green, G. G., & Ratcliff, G. G. (1989). Neurophysiological evidence of auditory channel anomalies in developmental dysphasia. Archives of Neurology, 46(8), 871-875.
3. Rabiner, L., Cheng, M., Rosenberg, A., & McGonegal, C. (1976). A comparative performance study of several pitch detection algorithms. IEEE Transactions on Acoustics, Speech, and Signal Processing, 24(5), 399-418.
4. Chen, N., & Hu, Y. (2007, August). Pitch detection algorithm based on Teager energy operator and spatial correlation function. In 2007 International conference on machine learning and cybernetics (Vol. 5, pp. 2456-2460). IEEE.
5. Bogert, B. P. (1963). The quefrency alanysis of time series for echoes; Cepstrum, pseudo-autocovariance, cross-cepstrum and saphe cracking. Time series analysis, 209-243.
6. Oppenheim, A. V., & Schafer, R. W. (2004). From frequency to quefrency: A history of the cepstrum. IEEE signal processing Magazine, 21(5), 95-106.
7. Rabiner L, Schafer R. Digital speech processing. TheFroehlich/Kent Encyclopedia of Telecommunications.2011;6:237–258.
8. Lathi, B. P., & Green, R. A. (2005). Linear systems and sig-

nals (Vol. 2). New York: Oxford University Press.
9. De La Cuadra, P., Master, A. S., & Sapp, C. (2001, September). Efficient pitch detection techniques for interactive music. In ICMC.
10. Atal, B. S. (1972). Automatic speaker recognition based on pitch contours. The Journal of the Acoustical Society of America, 52(6B), 1687-1697.
11. Gonzalez, S., & Brookes, M. (2011, August). A pitch estimation filter robust to high levels of noise (PEFAC). In 2011 19th European Signal Processing Conference (pp. 451-455). IEEE.
12. Talkin, D., & Kleijn, W. B. (1995). A robust algorithm for pitch tracking (RAPT). Speech coding and synthesis, 495, 518.
13. Ewender, T., Hoffmann, S., & Pfister, B. (2009). Nearly Perfect Detection of Continuous F_0 Contour and Frame Classification for TTS Synthesis. In Tenth Annual Conference of the International Speech Communication Association.
14. Atlas L, Janssen C. Coherent modulation spectral filtering for single-channel music source separation.In: Proceedings. (ICASSP'05). IEEE International Conference on Acoustics, Speech, and Signal Processing, 2005.. vol. 4. IEEE; 2005. p. iv–461.
15. Clark, P., & Atlas, L. (2009, April). A sum-of-products model for effective coherent modulation filtering. In 2009 IEEE International Conference on Acoustics, Speech and Signal Processing (pp. 4485-4488). IEEE.
16. Li, Q., & Atlas, L. (2008, March). Coherent modulation filtering for speech. In 2008 IEEE International Conference on Acoustics, Speech and Signal Processing (pp. 4481-4484). IEEE.
17. Moorer, J. (1974). The optimum comb method of pitch period analysis of continuous digitized speech. IEEE Transactions on Acoustics, Speech, and Signal Processing, 22(5), 330-338.
18. Zahorian, S. A., & Hu, H. (2008). A spectral/temporal method for robust fundamental frequency tracking. The Journal of the Acoustical Society of America, 123(6), 4559-4571.
19. Kawahara, H., Masuda-Katsuse, I., & De Cheveigne, A. (1999). Restructuring speech representations using a pitch-adaptive time–frequency smoothing and an instantaneous-frequency-based F0 extraction: Possible role of a repetitive structure in sounds. Speech communication, 27(3-4), 187-207.
20. Jurafsky D, Martin JH. Speech and languageprocessing: An introduction to natural language processing, computational linguistics, and speechrecognition (Second Edition). Pearson/ Prentice Hall Upper Saddle River; 2009.
21. W¨olfel M, McDonough JW. Distant speech recognition. Wiley Online Library; 2009
22. Rabiner, L. R., & Gold, B. (1975). Theory and application of digital signal processing. Englewood Cliffs: Prentice-Hall.
23. Standard of International Organization forStandardization. Acoustics — Normalequal-loudness-level contours. ISO 226:2003, Geneva CH. 2003;
24. Smith JO. Spectral Audio Signal Processing. Stanford University's Center for Computer Research in Music and Acoustics; 2011. http://ccrma.stanford.edu/jos/sasp/.
25. Bagshaw, P. (1993). Fundamental Frequency Determination Algorithm (FDA) Evaluation Database. Centre for Speech Technology Research, University of Edinburgh.
26. Mathworks. Estimate fundamental frequencyof audio signal. Matlab Docs R2019b. 2019;https://www.mathworks.com/help/releases/R2019b/audio/ref/pitch.html.
27. Hasanain AZ. Sqtpy Library. Python Package Index.2022; https://pypi.org/project/sqtpy
28. Fitch, W. T. (1997). Vocal tract length and formant frequency dispersion correlate with body size in rhesus macaques. The Journal of the Acoustical Society of America, 102(2), 1213-1222.
29. Albert, R. R., Schwade, J. A., & Goldstein, M. H. (2018). The social functions of babbling: acoustic and contextual characteristics that facilitate maternal responsiveness. Developmental science, 21(5), e12641.
30. Hoeschele, M. (2017). Animal pitch perception: Melodies and harmonies. Comparative Cognition & Behavior Reviews, 12, 5.
31. Warren, J. D., Uppenkamp, S., Patterson, R. D., & Griffiths, T. D. (2003). Separating pitch chroma and pitch height in the human brain. Proceedings of the National Academy of Sciences, 100(17), 10038-10042.
32. Bernhardsson E. Lang-pitch. GitHub. 2017;https://github.com/ erikbern/lang-pitch.
33. Kepuska, V. (2011). Wake-Up-Word Speech Recognition, Speech Technologies, Prof. Ivo Ipsic (Ed.), ISBN: 978-953-307-996-7, InTech.
34. Albert, R. R. (2013). Bidirectional influences of social feedback on parent-infant communication. Cornell University.
35. Chomsky N. Aspects of the Theory of Syntax.Cambridge, Mass: MIT Press. 1965;
36. Pisanski, K., Cartei, V., McGettigan, C., Raine, J., & Reby, D. (2016). Voice modulation: a window into the origins of human vocal control?. Trends in cognitive sciences, 20(4), 304-318.
37. Asiry, O., Shen, H., Wyeld, T., & Balkhy, S. (2018, July). Extending attention span for children ADHD using an attentive visual interface. In 2018 22nd International Conference Information Visualisation (IV) (pp. 188-193). IEEE.
38. Higuchi, S., Chaminade, T., Imamizu, H., & Kawato, M. (2009). Shared neural correlates for language and tool use in Broca's area. Neuroreport, 20(15), 1376-1381.
39. Mehrabian A. Nonverbal communication. Transaction Publishers; 1972.
40. Sun H. Confusing Double Consonant Sounds In Korean [TalkToMeInKorean]. TalkToMeInKorean.2016;https://youtu.be/Gg-VZxBIZjo
41. Green, J. A., Whitney, P. G., & Potegal, M. (2011). Screaming, yelling, whining, and crying: categorical and intensity differences in vocal expressions of anger and sadness in children's tantrums. Emotion, 11(5), 1124.